# Polymetallic sulphide mineralization in Chiplakot crystallines, northeast Kumaun Himalaya

**Rajesh Sharma*, Dinesh S. Chauhan and D. Rameshwar Rao**

Wadia Institute of Himalayan Geology, Dehra Dun 248 001, India

**We report here occurrence of polymetallic sulphide mineralization near Gasku, about 6 km north of Tawaghat in Kali valley. The minerals in the ore assemblage include chalcopyrite, pyrite, sphalerite, minor galena and pyrrhotite. They are present in the sericite–muscovite–talc–chlorite (± biotite) schist, and in the quartz veins present in these schists as well as in the amphibolite of the Chiplakot Crystalline Belt, localized in the vicinity of the North Chiplakot Thrust. The initial results of ore chemical and the fluid inclusions studies are presented, and a hydrothermal origin is plausible for this mineralization.**

**Keywords:** Chiplakot crystallines, fluid inclusions, Kumaun Himalaya, ore chemistry, polymetallic sulphides.

THE Chiplakot Crystalline Belt (CCB) in the northeast Kumaun Himalaya is a thrust slab which carries the rocks of Precambrian Indian crust – the Munsiari Formation that have been transported over the Lesser Himalayan metasedimentary sequence (Figure 1). It represents one of the many klippen of the Munsiari Formation, tectonically enthrusted and exhumed during the Himalayan orogeny. CCB is exposed along the Kali, Darma and Gori valleys, about 90 km north of Pithoragarh in Kumaun Himalaya. This is bounded by thrust designated as South Chiplakot Thrust in the south and North Chiplakot Thrust in the north, separating CCB from the tectonically underlying metasedimentary rocks of the Tejam Group/Berinag Formation of Lesser Himalaya[1]. Paul[2] believes that the South Chiplakot Thrust and North Chiplakot Thrust/Pangla Thrust are splays of the Munsiari Thrust, and that the CCB is not detached from the belt of Munsiari Formation since in its northwestern sector both are connected through a strip. To the east of Kali River in northwestern Nepal the Chiplakot crystallines extend to Seti River Valley[3]. The rocks of CCB include coarse gneissose granite, mylonitic porphyoblastic gneissose granite–granodiorite, augen gneisses, mica schists, fine-grained metasiltstone with interbedded sericite–chlorite schists, biotite–sericite–quartz schist, quartz porphyry and the bands of amphibolites. The rocks of CCB are metamorphosed up to amphibolite grade with their later retrogression. Various generation intrusion veins of microgranite, aplite, pegmatite and quartz are also present predominantly in the gneissose granite. Veins showing both concordant and cross-cutting relation with the schistosity are present, and oblique veins are not uncommon. Patel and Kumar[4] believe that the two major geotectonic regime, viz. an early Himalayan ductile and a superimposed brittle deformation broadly acted for the evolution of CCB. A whole rock Rb–Sr age of 1906 ± 220 ma to the gneisses of Tawaghat area[5], and 1830 ± 200 ma to the Munsiari Formation from near CCB[6] have been assigned. The sedimentary sequence of the Lesser Himalaya lying in contact with CCB is largely the rocks of Tejam Group, with a band of the Berinag Formation exposed in the northeastern boundary of CCB[1]. They comprised of schistose quartzite with interbedded amphibolites, carbonaceous phyllites and the limestone. Earlier investigations on CCB mainly include accounts of its geology and structural evolution particularly on a regional scale[1,2,7–12].

A zone of sulphide mineralization has been noticed recently at the northern border of Chiplakot crystallines along the North Chiplakot Thrust, about 100 m north of Gasku village. Herein, the North Chiplakot Thrust forms the boundary between southerly located Chiplakot crystallines and the northern Berinag Formation. The mala-

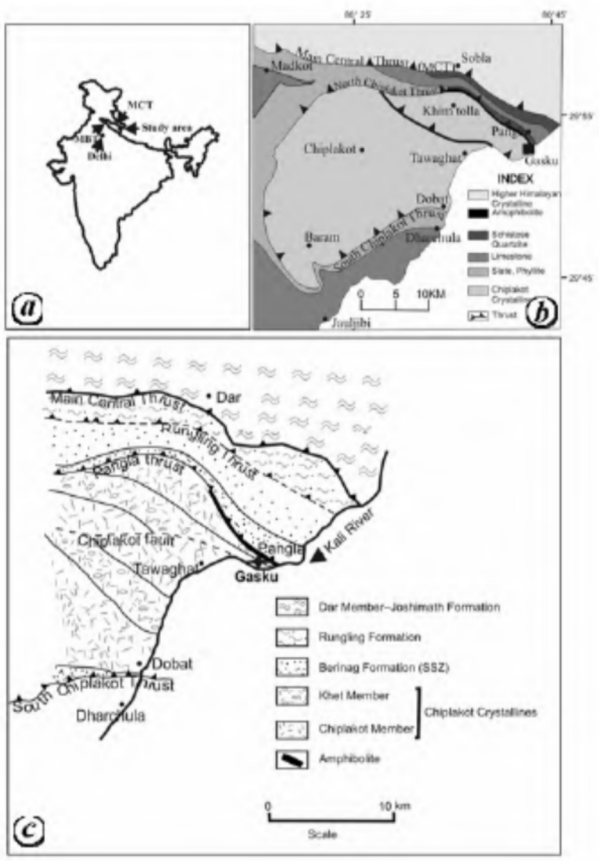


**Figure 1.** *a*, Location map of the study area. *b*, Geological map of the Chiplakot klippe[4] showing location of the Gasku mineralization. *c*, Geological map of section between Dobat–Pangla[2].

*For correspondence. (e-mail: sharmarajesh@wihg.res.in)

chite is seen sporadically on the schists over a width of about 250 m. Some specks of cuprite are also noted. Their encrustations on the host schistose rocks are sprinkled and at times patchy (Figure 2 *a*). The mineral assemblage observed under the microscope consists of chalcopyrite, pyrite, sphalerite, minor pyrrhotite, and secondary azurite and covelite. Quartz forms the ubiquitous gangue mineral. The encrustations of the altered zone of mineralization are present in the intensely folded sericite–muscovite–talc–chlorite schist, sericite–chlorite–biotite–quartz schist of the Chiplakot crystallines. Mineralized quartz veins occur commonly parallel to the schistosity. Within such quartz veins, specks of sulphide minerals are observed. Nodules of quartz encircled by the micaceous minerals are at times developed linked to these veins. In addition, amphibolite is present along the thrust and the veinlets of quartz consisting sulphide mineralization are observed in the fractures of this amphibolite. Mineralized veins in the amphibolite are random-oriented. Oblique quartz veins are also present but except for signs of malachite leaching, sulphide mineral specks are not seen in these veins. The mineralized zone is restricted to the North Chiplakot Thrust and encrustations of alteration zone and specks do not traverse laterally. The foliation parallel arrangement of the veins could be because of their orientation along the weak planes restricted to the trust zone. Their perfect relation with metamorphism is lacking and mineralization is likely a thrust controlled phenomena. However, malachite encrustations, chalcopyrite, covelite associated with quartz gangue are also seen on the granitic gneiss of Chiplakot crystallines near Raungti nala between Dobat and Tawaghat section, about 8 km south of Tawaghat. Near this encrustation, specks of chalcopyrite and pyrite are also noticed within the granitic gneiss. A sample from this location showed that chalcopyrite is the main primary sulphide followed by associated pyrite under the microscope.

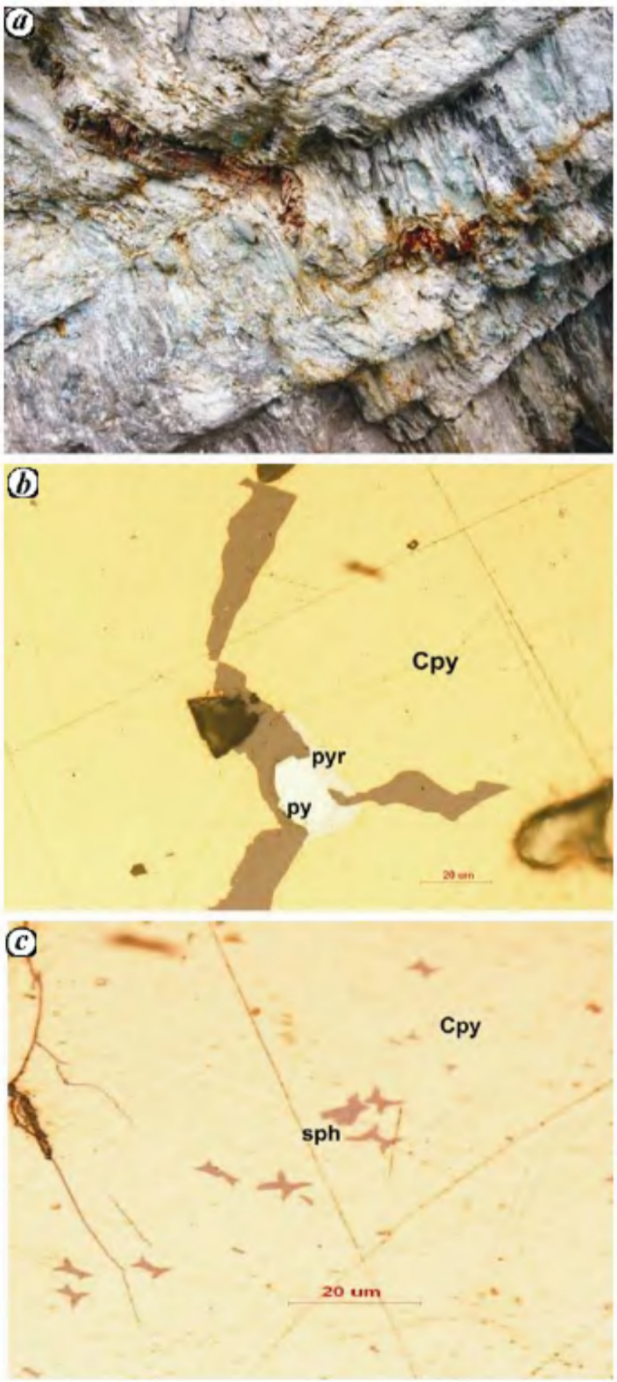


**Figure 2.** ***a***, Field photograph showing malachite encrustation near Gasku. ***b***, Photomicrograph showing coeval pyrite and pyrrhotite replaced by chalcopyrite. ***c***, Star-like and skeletal sphalerite in chalcopyrite.

Limited ore petrography shows that chalcopyrite and pyrite are dominant minerals followed by sphalerite, pyrrhotite and rare galena grains. These ore minerals show intimate relation with the gangue quartz as both are infilled in the fractures. Chalcopyrite is seen as irregular aggregates, whereas sphalerite is present as thin veinlets and small articles associated with chalcopyrite. Chalcopyrite of two generations is present – early chalcopyrite shows coeval boundary with pyrite while the late chalcopyrite replaces coeval pyrite and pyrrhotite (Figure 2 *b*). Characteristic dot-like and star-like sphalerite is noticed in chalcopyrite (Figure 2 *c*). Fine skeletal sphalerite is also observed in the chalcopyrite. Experimental studies[13] suggest that such sphalerite in chalcopyrite begins to dissolve at 400°C. Thus they were possibly formed at <400°C from a cooling high temperature ore solution. Such features of sphalerite in chalcopyrite are considered to be products of exsolution of sphalerite from primary chalcopyrite or from intermediate solid solution[14]. They may be found in high temperature chalcopyrite formed from hydrothermal or pyrometasomatic systems. The SEM-EDX analysis of the surface weathered sample of host schist from near Gasku has been carried out using Bruker-make EDX equipped with $LN_2$ free SDD X flash 4010 detector and Zeiss EVO-40 EP micro-

**Table 1.** Representative EPMA data of the sulphide minerals from Gasku

| Elements (%) | Chalcopyrite (average of 14 analyses) | Pyrite (average of 11 analyses) | Sphalerite (average of 9 analyses) |
|---|---|---|---|
| S | 34.359 | 38.937 | 33.173 |
| V | 0.021 | 0.007 | 0.026 |
| Mn | 0.006 | 0.011 | 0.013 |
| Fe | 30.966 | 58.754 | 10.435 |
| Co | 0.008 | 0.111 | 0.052 |
| Ni | 0.017 | 0.593 | 0.008 |
| Cu | 33.432 | 0.024 | 0.799 |
| Zn | 0.077 | 0.152 | 52.644 |
| Mo | 0.504 | 0.545 | 0.508 |
| Cd | 0.029 | 0.017 | 2.263 |
| Total | 99.419 | 99.152 | 99.921 |

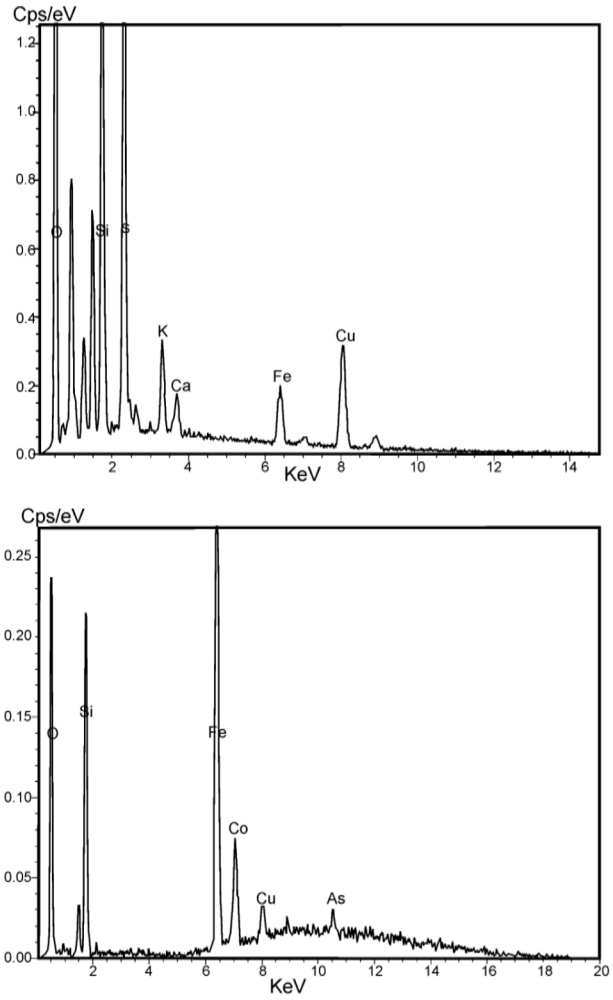


**Figure 3.** SEM-EDX analyses diagrams showing presence of Cu, Fe, Co, As in Gasku weathered zone.

scope at the SEM laboratory of WIHG. A number of spot analyses and the line scans are performed at 20 kV current. The results of two of them are shown in Figure 3 *a* and *b*. These results show presence of Cu, Fe, Co, Zn, Pb and As in the weathered zone of sulphide mineralization. Indication of the presence of minor Sn is also noticed in one of the records. Cu and Fe with distinct peaks are most common elements of interest.

Chalcopyrite, pyrite and sphalerite from Gasku are quantitatively analysed using Cameca SX100 super probe at WIHG EPMA laboratory and under comparable operating conditions: 15 kV accelerating voltage, 20 nA probe current and 2 μm beam size. The analyses in general showed the presence of S, Cu, Fe, Zn as major elements and Cd, Mo, Mn, Co and Ni, as trace elements. A total number of 14 spots are analysed for chalcopyrite, 11 for pyrite and 9 for sphalerite. The average of these analyses for each of the minerals is given in Table 1. Chalcopyrite shows an average 0.5 wt% Mo, 770 ppm Zn and 290 ppm of Cd. High concentration of Zn in chalcopyrite and vice versa is attributed to solid solution between chalcopyrite and sphalerite. Also that $a_{Zn}^{2+}$ in the ore forming fluid was high as indicated by high Zn concentration in pyrite and chalcopyrite and the presence of sphalerite in mineral assemblage. The Mo is invariably distributed in all the analysed minerals whereas concentrations of Co and Ni are higher in pyrite than in chalcopyrite. Although significant Co is present in pyrite, the concentration of Ni is much higher, thereby the Co/Ni ratios are low. Unlike the pyrites from Ramgarh Formation[15], Ni is always higher than Co in the pyrite from Gasku. Since the concentration of Co, Ni and their ratios in pyrite have consequence in understanding the genesis of ores[16], present data can be compared with such records from various genetic types of ores. Pyrite contains an average 1110 ppm Co and 5930 ppm Ni presenting an average 0.19 Co/Ni ratios. Majority of the data provided >0.2 values with four analyses, suggesting <0.2 Co/Ni ratios. In spite of such Co/Ni ratios in pyrite, the very high concentrations of Ni and Co advocate a magmatic environment for the formation of this pyrite. Our data match well with some Czech-Slovakian deposits[17] of magmatic affinity. Further, envisaged work including evaluation of Ni contents in the country rocks may be more useful. Sphalerite is characterized by high Fe and Cd concentration. Fe contents in

**Table 2.** Fluid inclusion data of the mineralized quartz from Gasku sulphide mineralization

| Inclusion type | Temperature of $CO_2$ melting (°C) | Temperature of final ice melting (°C) | Temperature of $CO_2$ homogen (°C) | Temperature of homogen (°C) |
|---|---|---|---|---|
| Saline-aqueous | – | –6.7 to –9.3 | – | 258 to 316 |
| Aqueous-carbonic | –57.6 to –56.8 | – | +24.1 to +30.1 | 280 to 349 |

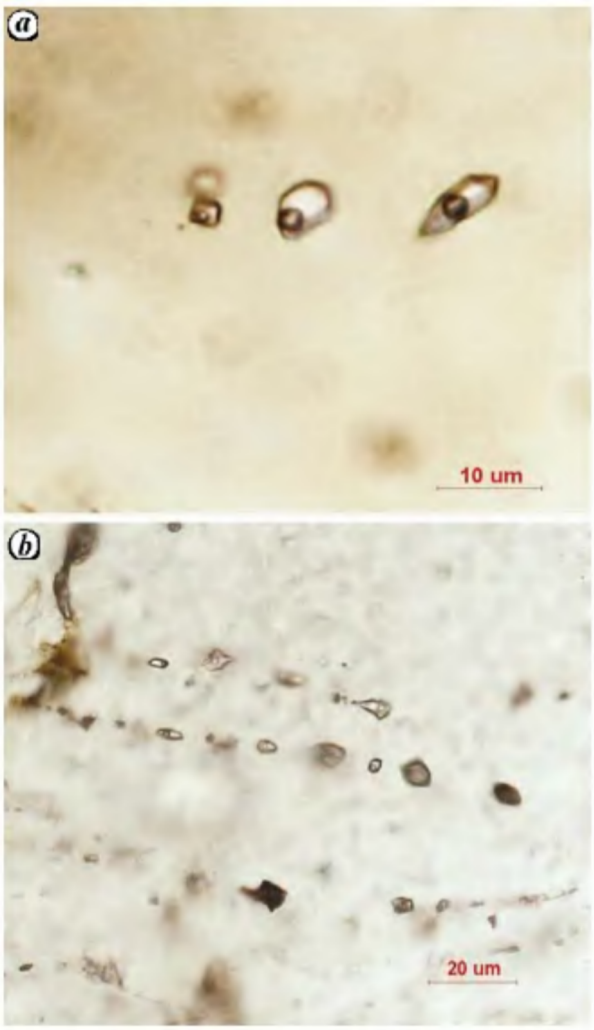


**Figure 4.** Photomicrographs of the fluid inclusions observed in the mineralized quartz veins from Gasku. ***a***, Biphase aqueous inclusions. ***b***, Coexisting aqueous-carbonic and biphase aqueous inclusions.

sphalerite vary between 9.8 and 10.8 wt%, and with an average of 10.43 wt%. This sphalerite is enriched in Cd with an average 2.26 wt% Cd content. Sphalerite consists of about 0.8 wt% Cu, 0.5 wt% Mo and an average 130 ppm Mn. Lin and Tiegeng[18] reported average 1.38% Cd in sphalerite from the Niujiaotang Cd-rich zinc deposit of China. However, the average Cd contents of sphalerite in different types of ore deposits vary between 0.2 and 1.0 wt%[19]. In the present case, high Cd is likely to be present as isomorphous impurity in sphalerite resulting from the substitution of $Zn^{2+}$. High concentration of metals like Fe, Cd, Cu and Mo in sphalerite is generally related to the formation temperature, metal source and amount of sphalerite in ores[19]. Considering that they are generally higher in skarn and hydrothermal ores, the present higher concentration may point to a hydrothermal nature of the studied mineralization.

The fluid inclusion study on the mineralized quartz veins is carried out at WIHG Fluid Inclusion Lab. Microthermometry is performed using calibrated Linkam THMSG 600 fluid inclusion stage fitted onto Nikon E600 microscope. Data presented here (Table 2) is correct within ±0.2°C at sub-ambient temperatures and ±3°C at the total homogenization temperatures. Flincor computer program of Brown[20] has been used for the fluid inclusion calculations. Three types of fluid inclusions are present in the studied samples: (i) A prominent event of the fluid participation is represented by the saline aqueous inclusions (Figure 4 *a*) with 70–90 vol% aqueous liquid and a contemporary vapour bubble. They are present in isolated random distribution and in small arrays that are well restricted to single grain. They are commonly 5–15 micron in size and semiround or semiregular in shape. The eutectic temperatures of the trapped fluid vary from –24.8°C to –27.1°C suggesting its composition: $H_2O$–NaCl–KCl with minor presence of Mg/Ca in this fluid. The final melting of ice in the frozen aqueous inclusions occur at –6.7°C to –9.3°C, which is consistent with the salinity of 10.11 to 13.8 wt% eqiv. NaCl. These inclusions are homogenized between 258°C and 316°C invariably to the liquid phase. (ii) Another event of the aqueous fluid circulation is represented by small <5 micron size, semiround biphase inclusions present in secondary trails. The proportion of liquid–vapour filled within them is about 90 : 10. They are not widespread and show homogenization at 160 ± 10°C. (iii) Aqueous-carbonic inclusions (Figure 4 *b*) are also present in gangue quartz. The proportion of the aqueous and carbonic phase is highly inconsistent from 90 : 10 to 60 : 40, coupled with the uncommon presence of up to 80 vol% carbonic phase. These inclusions show a distribution pattern near similar to that of aqueous inclusions, at times both coexisting in single array, in a single grain (Figure 4 *b*). But the population of these inclusions is low with only about 30% of the aqueous inclusion's population. They are also semiregular in shape and 10 ± 5 micron in size. Melting of carbonic phase occurs between –57.6°C and –56.8°C, confirming that the carbonic fluid is $CO_2$ and only <6 mol% $CH_4$ is expected. The $CO_2$ phase homogenization to liquid $CO_2$ at a temperature range of +24.1°C to +30.1°C

suggests a low $CO_2$ density: 0.73–0.59 g/cm$^3$. The complete homogenization of these inclusions occurs in a range of 280–349°C to the aqueous phase. The composition of their aqueous phase is similar to type I aqueous fluid as indicated by eutectic temperatures (cf. $-25 \pm 2$°C) in 3–4 $H_2O$–$CO_2$ inclusions.

Considering that only the mineralized quartz with disseminated ore has been used for fluid inclusion study, and that the types I and III inclusions are primary as per their distribution features, it is suggested that overall a $H_2O$–$CO_2$ fluid was present during ore formation. Further, contemplation of microthermometric study implies a dominance of aqueous component with $H_2O$–NaCl–KCl ± Mg/Ca composition, and a low $XCO_2 = 0.138$ in the trapped fluid. Primary nature of the fluid inclusions and the localized occurrence of mineralized veins also indicate that this brine-rich fluid was active in the thrust zone. A low estimated density of $CO_2$ when compared with the earlier records of $CO_2$ density (average 0.86 g/cm$^3$) from equivalent rocks of Munsiari Formation[22,23] argue that the aqueous-carbonic fluid characterized here is not the peak metamorphic fluid. The flux of mineralizing fluid along the thrust possibly occurred during the uplift, though more evidences based on envisaged study may be conclusive. This upper range of homogenization temperature obtained and the dominant brine fluid indicate that the fluid involved is likely to be hydrothermal. The perception is also convincing considering that the metamorphic fluids reported from the equivalent crystalline rocks in Himalaya are $CO_2$ rich. The ore replacement and exsolution features and the chemical evidence also favour that the ore was deposited from a high temperature cooling system. Arrival of a late aqueous fluid in the fine fractures developed in quartz suggests that the mineralization event was not the closing stage of the fluid activity in the area. Type II inclusions document the late lower temperature aqueous fluid migration through the North Chiplakot Thrust. Overall, this occurrence of sulphide minerals at Gasku is significant in view of their similarities in tectonic setting and depositional features with the known Askot polymetallic sulphide deposit in an adjacent analogous klippe rocks – the Askot Crystalline[24].


1. Validya, K. S., *Geology of Kumaun Lesser Himalaya*, The Himachal Times Press, Dehradun, India, 1980, p. 291.
2. Paul, S. K., Geology and tectonics of the Central Crystallines of northeastern Kumaon Himalaya, India. *J. Nepal Geol. Soc.*, 1998, **18**, 151–167.
3. Bashyal, R. P., Geological framework of far western Nepal. *Him. Geol.*, 1984, **12**, 40–50.
4. Patel, R. C. and Kumar, Y., Late-to-post collisional brittle-ductile deformation in the Himalayan orogen: evidences from structural studies in the Lesser Himalayan Crystalline, Kumaon Himalaya, India. *J. Asian Earth Sci.*, 2006, **27**, 735–750.
5. Singh, V. P., Bhanot, V. B. and Singh, R. P., Geochronology of the granitic and gneissic rocks from Munsiari, Namik and Tawaghat areas of the Central Crystalline Zone, Kumaun Himalaya, UP. Pre-print presented at the Third National Symposium on Mass Spectrometry, Hyderabad, 22–24 September 1985.
6. Bhanot, V. B., Singh, V. P., Kansal, A. K. and Thakur, V. C., Early Proterozoic Rb–Sr whole rock age for Central Crystalline gneiss of Higher Himalaya, Kumaun. *J. Geol. Soc. India*, 1977, **18**, 90–91.
7. Powar, K. B., Petrology and structure of Central Crystalline Zone, northeastern Kumaun. *Him. Geol.*, 1972, **2**, 34–46
8. Mehdi, S. H., Kumar, G. and Prakash, G., Tectonic evolution of eastern Kumaun Himalaya: a new approach. *Him. Geol.*, 1972, **2**, 481–501.
9. Thakur, V. C. and Choudhary, B. K., Deformation, metamorphism and tectonic relations of Central Crystalline and Main Central Thrust in eastern Kumaun Himalaya. *Himalayan Shears* (ed. Saklani, P. S.), Himalayan Books, New Delhi, 1983, pp. 45–57.
10. Valdiya, K. S., Tectonic and evolution of central sector of the Himalaya. *Philos. Trans. R. Soc. London*, 1988, **A326**, 151–175.
11. Dubey, A. K. and Paul, S. K., Map pattern produced by thrusting and subsequent superposed folding: model experiment and example from the NE-Kumaon Himalayas. *Eclogae Geol. Helv.*, 1993, **86**, 839–852.
12. Patel, R. C., Kumar, Y., Nand Lal and Kumar, A., Thermotectonic history of the Chiplakot Crystalline Belt in the Lesser Himalaya, Kumaon, India: constraints from apatite fission-track thermochronology. *J. Asian Earth Sci.*, 2007, **29**, 430–439.
13. Sugaki, A. and Tashiro, C., Thermal studies on the skeletal crystals of sphalerite in chalcopyrite. *Sci. Rep. Tohoku Univ.*, 1957, 293–304.
14. Sugaki, A., Kitakaze, A. and Kojima, S., Bulk compositions of intimate intergrowths of chalcopyrite and sphalerite and their genetic implications. *Mineral. Deposita*, 1987, **22**, 26–32.
15. Sharma Rajesh, Sulphide mineralization in uprising Lithotectonic Belt of Lesser Himalaya. In *Magmatism, Tectonism and Mineralization* (ed. Santosh Kumar), Macmillan Publishers, New Delhi, 2009, pp. 230–246.
16. Bajwah, Z. U., Seccombe, P. K. and Offler, R., Trace element distribution, Co–Ni ratios and genesis of Big Cadia iron–copper deposit, New South Wales, Australia. *Mineral. Deposita*, 1987, **22**, 292–300.
17. Cambel, B. and Jarkovsky, J., Geochemistry of nickel and cobalt in pyrrhotines of different genetic types. 23rd International Geologists Congress, 1968, vol. 6, pp. 169–183.
18. Lin, Ye and Tiegeng, Liu, Sphalerite chemistry, Niujiaotang Cd-rich zinc deposit, Guizhou, southwest China. *Chinese J. Geochem.*, 1999, **18**, 62–68.
19. Cook, N. J. *et al.*, Trace and minor elements in sphalerite: a LA-ICPMS study. *Geochim. Cosmochim. Acta*, 2009, **73**, 4761–4791.
20. Brown, P. E., FLINCOR: a microcomputer program for the reduction and investigation of fluid inclusion data. *Am. Min.*, 1989, **79**, 1390–1393.
21. Bodnar, R. J., Revised equation and table for determining the freezing point depression in $H_2O$–NaCl solutions. *Geochim. Cosmochim. Acta*, 2003, **57**, 683–684.
22. Sachan, H., Sharma, R., Sahai, A. and Gururajan, N. S., Fluid events and exhumation history of the Main Central Thrust zone Garhwal Himalaya (India). *J. Asian Earth Sci.*, 2001, **19**, 207–221.
23. Sharma, R. and Lal, S. N., Metamorphic and fluid evolution across the MCT zone: evidences from the metapelites in Kumaun Himalaya. National Seminar on Active and Fossil Suture Zones, Dehra Dun, 22–23 November 2006, p. 94.
24. Ghose, A., A note on the polymetallic sulphide mineralization in Askot area, Pithoragarh district, Uttar Pradesh. *Rec. Geol. Surv. India*, 1976, **107**, 1–11.


ACKNOWLEDGEMENTS. We thank Prof. B. R. Arora, Director, WIHG, for permission to publish this paper and for the encouragement received. We acknowledge help of Dr N. K. Saini and Shri Naresh Juyal in SEM-EDX work. We also thank the anonymous reviewer for helpful suggestions.

Received 26 May 2008; revised accepted 27 January 2010